Organic & Biomolecular Chemistry

RSC Publishing

PAPER

View Article Online
View Journal | View Issue

Cite this: *Org. Biomol. Chem.*, 2013, **11**, 5683

Bisacenaphthopyrazinoquinoxaline derivatives: synthesis, physical properties and applications as semiconductors for n-channel field effect transistors†

Chenhua Tong,[a] Jingjing Chang,[a] Jun Min Tan,[a] Gaole Dai,[a] Kuo-Wei Huang,[b] Hardy Sze On Chan*[a] and Chunyan Chi*[a]

Received 9th May 2013,
Accepted 4th July 2013

DOI: 10.1039/c3ob40982a

www.rsc.org/obc

Several bisacenaphthopyrazinoquinoxaline (BAPQ) based derivatives **1–3** were synthesized by condensation between the acenaphthenequinones and 1,2,4,5-tetraaminobenzene tetrahydrochloride. Their optical, electrochemical and self-assembling properties are tuned by different substituents. Among them, compound **3** possesses a homogeneously distributed low-lying LUMO due to the peripheral substitution with four cyano groups. The corresponding n-channel field effect transistors showed a field effect electron mobility of 5×10^{-3} cm^2 V^{-1} s^{-1}.

Introduction

Introduction of an imine nitrogen atom into the framework of acenes has become an efficient way to stabilize this type of unstable molecule. At the same time, due to the increased electron affinity,[1] they can be used as potential n-type semiconducting materials.[2–4] Depending on the number and positions of nitrogen atoms in the acene framework, different electronic structures, stability, solubility, and molecular packing can be achieved.[5] Although many syntheses and theoretical calculations on aza-acenes have been conducted, there are still a limited number of *N*-heteroacenes that can be successfully used in electronic devices such as organic field effect transistors (OFETs), especially when processed from solutions.[2l,m]

A pyrazine ring is the most widely utilized moiety to construct *N*-heteroacenes owing to its convenient synthesis by condensation reactions.[6] However, pyrazinacenes with a high pyrazine unit density are hard to obtain because they are very sensitive to even weak nucleophiles.[7] Incorporation of other electron-withdrawing groups into a pyrazinacene is therefore effective for a higher electron affinity.[2l,m,3] A fused five-membered ring can lower the LUMO energy level of an acene framework due to its tendency to accept an electron through aromatic $4n + 2$ stabilization. Furthermore, introduction of a five-membered ring also causes a two-dimensional fusion, which further stabilizes the π-system. Stable and soluble acene derivatives containing both pyrazine units and five-membered rings are therefore of interest. They can be achieved through a condensation reaction between arene diamine and acenaphthenequinone. Herein, we report the development of several bisacenaphthopyrazinoquinoxaline (BAPQ) based candidates **1–3** (Fig. 1) and investigate their potential application in n-channel OFETs. As an analogue of 5,7,12,14-tetraazapentacene, BAPQ has a larger area for packing, a slightly lower LUMO energy level and a much higher stability,[8] but an increased reorganization energy in principle.[9] Recently, the linear and star-shaped BAPQ derivatives with imide groups have been synthesized and proposed as the n-type semiconductors.[3d] However, their FET performance has not been reported. In this paper, three molecules based on BAPQ have been synthesized and used for OFET applications by solution processing techniques. Two types of solubilizing functional groups were adopted to improve the solubility: (i) flexible aliphatic chains on the naphthalene edges (compound **1**) and (ii) the alkylphenyl group in the middle edges (compounds **2** and **3**). The

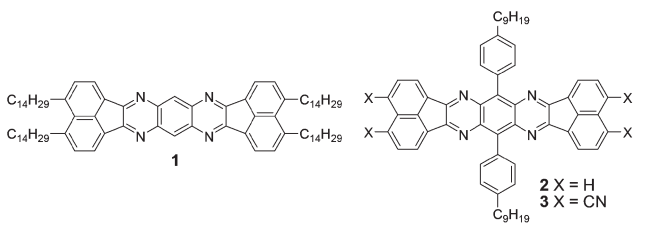

Fig. 1 Structures of BAPQ derivatives **1–3**.

[a]*Department of Chemistry, National University of Singapore, 3 Science Drive 3, Singapore, 117543, Singapore. E-mail: chmcsoh@nus.edu.sg, chmcc@nus.edu.sg; Fax: +65 6779 1691; Tel: +65 6516 5375*
[b]*KAUST Catalysis Center and Division of Chemical and Life Sciences and Engineering, 4700 King Abdullah University of Science and Technology, Thuwal 23955-6900, Kingdom of Saudi Arabia*

†Electronic supplementary information (ESI) available: Structural characterization data for all new compounds; DFT calculation data; additional electrochemical data; TGA curves and thin film XRD data. See DOI: 10.1039/c3ob40982a

four strong electron-withdrawing cyano groups in **3** are expected to further lower the LUMO energy level and reduce the inner reorganization energy.[5] The target compounds have good stability and solubility, and their photophysical properties, electrochemical properties, thermal behaviours, and OFET activities are studied in detail in this work.

Results and discussion

Synthesis

The synthesis of compound **1** started from the protection of 5,6-dibromoacenaphthylene-1,2-dione **4**[10] by ethylene glycol to give compound **5** in 45% yield (Scheme 1). Subsequent Hagihara–Sonogashira coupling between **5** and 1-tetradecyne gave compound **6** in 77% yield. Hydrogenation of the alkyne groups in compound **6** was then conducted using hydrazine over Pd/C to afford the dialkylated compound **7** in 34% yield. Herein, Kumada coupling reaction was also attempted to directly prepare compound **7** from **5** using saturated aliphatic Grignard reagent, but resulted in a failure presumably due to the steric hindrance caused by the two neighbouring bromo groups. The *p*-toluenesulfonic acid-catalyzed deprotection of **7** was carried out in a mixed solvent (water, acetonitrile (AN) and dichloromethane (DCM)) to give **8** in quantitative yield. BAPQ derivative **1** was finally obtained through the acid-catalyzed condensation between acenaphthenequinone **8** and the 1,2,4,5-tetraaminobenzene tetrahydrochloride **9**[11] in 70% yield.

The syntheses of compounds **2–3** started from the Stille coupling between 4,7-dibromo-5,6-dinitrobenzothiadiazole **10**[12] and 4-nonylphenyl trimethyl stannane **11**[13] to give the dinitrobenzothiadiazole **12** in 71% yield (Scheme 2). Reduction of **12** by Zn/HOAc led to an air-sensitive intermediate tetraamine **13**, which reacted with the quinone **14a** and **14b**[14] to give BAPQ derivatives **2** and **3** in overall 46% and 13% yield, respectively. Compound **2** can be prepared from **12** in a one-pot reaction without the purification of intermediate **15**. However, the separation of intermediate **16** was necessary for further reaction and the reaction yield was low (28%), which is due to the decomposition of the cyano groups in the presence of Zn/HOAc and the incomplete reduction of **12**. The condensation between **16** and **14b** finally gave pure compound **3** in 48% yield.

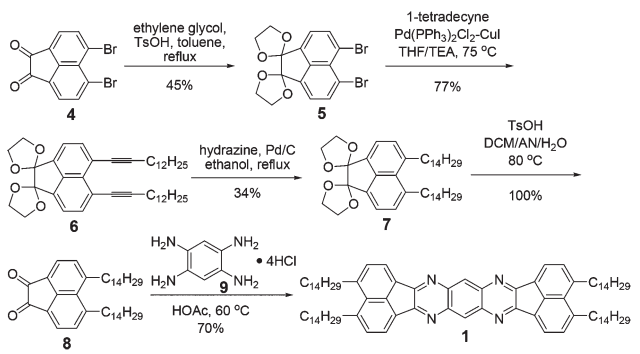

Scheme 1 Synthetic route of BAPQ derivative **1**.

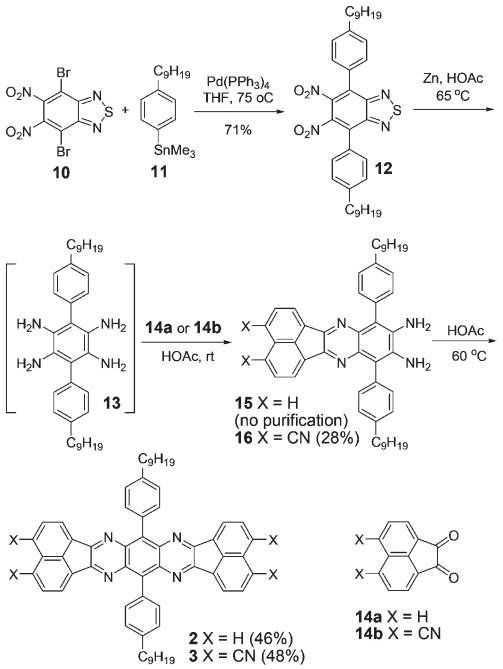

Scheme 2 Synthetic route of BAPQ derivatives **2–3**.

The chemical structures of compounds **1–3** and intermediates are identified by NMR, MALDI-TOF mass spectra and elemental analysis (see ESI†). Because of the strong aggregation, compound **1** has a poor solubility in most organic solvents at room temperature, but it can be dissolved in hot toluene. Compound **2** is well dissolved in chlorinated or aromatic solvents, and compound **3** shows a good solubility in chlorobenzene.

Photophysical properties

The UV-Vis absorption and fluorescence spectra recorded in dilute toluene solution and a thin film are shown in Fig. 2, and the data are summarized in Table 1. At a concentration of 1.0×10^{-5} M in toluene solution, compound **1** shows a broad absorption band at room temperature (see Fig. S1 in ESI†) which is consistent with the spectrum of **1** in a thin film form. This similarity is caused by the strong tendency of **1** to form aggregates in solution. If the solution is heated to 80 °C, the absorption band becomes sharp with an absorption maximum at 378 nm (Fig. 2a), indicating that the aggregation is reduced at high temperature. This aggregation effect can be also observed from its ^{1}H NMR spectrum. At room temperature, no signal related to aromatic protons can be observed in many organic solvents such as $CDCl_3$ and $CDCl_2CDCl_2$. However, the sharp peaks appear between 7.7 and 9.1 ppm when the $CDCl_2CDCl_2$ solution is heated to 100 °C. This further confirms that the aggregates are suppressed at high temperature. At room temperature, compounds **2** and **3** just display a narrow intense absorption band with λ_{max} at 376 nm and 397 nm, respectively, due to the suppressed aggregation by the

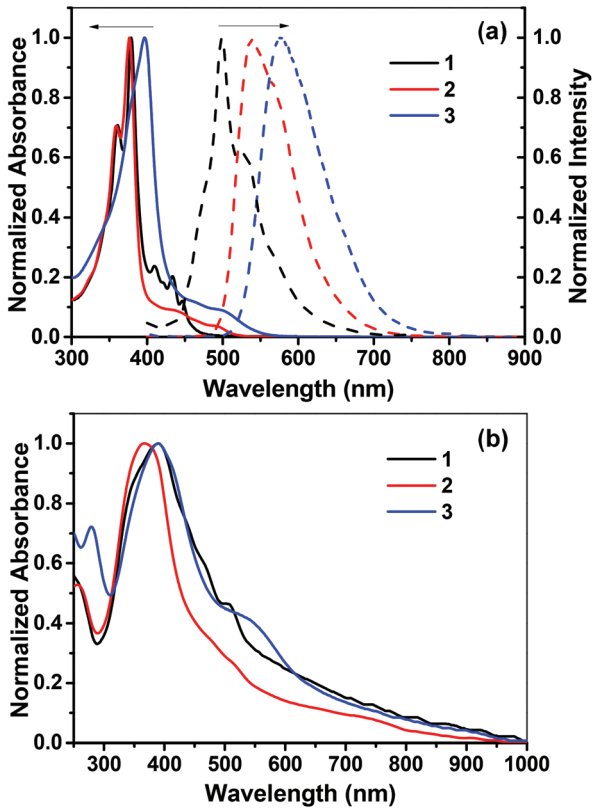

Fig. 2 (a) Normalized UV-Vis absorption and fluorescence spectra of **1–3** in toluene (the spectra of compound **1** were recorded at 80 °C, all of the fluorescence spectra were recorded with excitation wavelength at their absorption maximum). (b) Normalized UV-Vis absorption spectra of **1–3** in thin films.

alkylphenyl substituents. The optical band gap extracted from the low-energy absorption edge is 2.70, 2.37 and 2.25 eV for compounds **1–3**, respectively. In thin films, the absorption spectra of compounds **1–3** significantly become broader with long tails to the near-IR region and show slight hypsochromic shifts (at λ_{max}) compared to that in solutions, indicating strong intermolecular associations in the solid state. Compounds **1–3** show sharp fluorescence spectra in toluene (at 1.0×10^{-6} M) with emission maxima at 499, 538 and 579 nm, respectively. In the solid state, no fluorescence can be observed for all of these compounds due to the strong aggregation.

Electrochemical properties

Cyclic voltammetry (CV) and differential pulse voltammetry (DPV) measurements were conducted for **1–3** in chlorobenzene

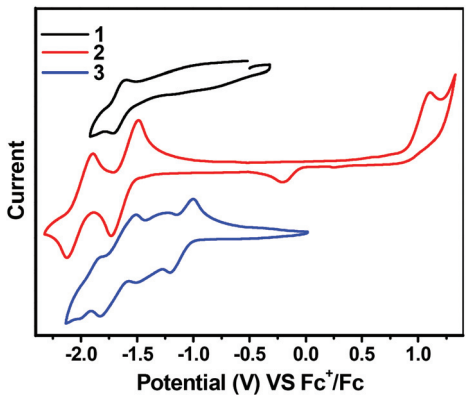

Fig. 3 Cyclic voltammograms of BAPQ derivatives **1–3** in chlorobenzene at a concentration of 1×10^{-3} M (curve of **1** was recorded at 80 °C).

(Fig. 3 and Fig. S2 in ESI†) and the data are summarized in Table 1. Due to strong aggregation, the voltammogram of compound **1** was recorded at elevated temperature (80 °C), but only one weak redox wave was observed, with half-wave potential $E_{1/2} = -1.65$ (*vs.* Fc^+/Fc). For compound **2**, two pairs of pyrazine-based reversible reduction waves at $E_{1/2} = -2.02$ and -1.63 V and one naphthalene-based irreversible oxidization wave at $E_{1/2} = 1.01$ V were observed with a band gap of 2.44 eV. A small peak at -0.20 V corresponds to the reduction of an irreversibly oxidized product from compound **2** on the electrode surface. Compound **3**, as a structure designed for high electron affinity, exhibits four pairs of reduction waves at $E_{1/2} = -1.90$, -1.70, -1.38 and -1.09 V, respectively. The LUMO energy levels of these BAPQ derivatives are determined to be -3.27 eV for **1** and **2**, and -3.78 eV for cyanide **3**, from the onset of the first reduction wave. They all exceed the suggested value (<-3.15 eV) to allow an n-channel operation of OFETs.[4a]

TD DFT calculations

Time-dependent density functional theory (TD DFT at B3LYP/6-31G*)[16] calculations were conducted for compounds **1–3** to understand their electronic and optical properties by using Gaussian 09[17] (see details in ESI†). All the solubilizing aliphatic chains were displaced by ethyl groups to simplify the calculation. The geometries of these molecules were fully optimized in the gas phase using the default convergence criteria without any constraints and confirmed by frequency calculations. The LUMO orbitals of compounds **1–2** are mainly

Table 1 Summary of photophysical and electrochemical properties of **1–3**[a]

	$E_{1/2}$/V	HOMO/eV	LUMO/eV	E_g/eV	E_g^{opt}/eV	$\lambda_{max}^{abs\ c}$/nm	ε/cm^{-1} M^{-1}	$\lambda_{max}^{emi\ d}$/nm	$\lambda_{max}^{abs\ e}$/nm
1	−1.65	−5.97[b]	−3.27	—	2.70	378	53 000	499	390
2	−2.02, −1.63, 1.01	−5.71	−3.27	2.44	2.37	376	237 600	538	366
3	−1.90, −1.70, −1.38, −1.09	−6.03[b]	−3.78	—	2.25	397	155 000	579	390

[a] HOMO and LUMO energy levels were determined from the onset of the first oxidation and reduction wave according to the equations: HOMO = $-(4.8 + E_{ox}^{onset})$ eV and LUMO = $-(4.8 + E_{red}^{onset})$ eV.[15] [b] Calculated according to the equation: HOMO = LUMO − E_g^{opt}. [c] In dilute toluene solution (1.0×10^{-5} M). [d] In dilute toluene solution (1.0×10^{-6} M). [e] In thin film.

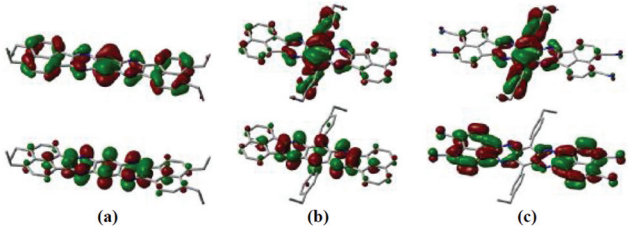

Fig. 4 HOMO (up) and LUMO (down) profiles of BAPQ derivatives (a) **1**, (b) **2** and (c) **3**.

distributed in the central aza-anthracene moiety (Fig. 4). Owing to the four strong π electron-withdrawing cyano groups, the LUMO of **3** is mainly localized in the two side parts of the central benzene ring, which may enhance intermolecular electronic coupling in the solid state. The HOMO orbital of molecule **1** is homogeneously distributed, while it is mainly localized at the central phenyl benzene rings for molecules **2** and **3**. The partially separated frontier orbital profiles of molecule **3** indicate significant intramolecular charge transfer character. This is the reason why the absorption and emission spectra of compound **3** show an obvious red-shift compared to that of molecules **1** and **2**. Accordingly, compound **2** also has a weak intramolecular charge transfer character. The calculated absorption data predicted a major absorption band at 366 nm (oscillator strength f = 3.1295) for **1**, three bands at 462, 365, 276 nm (f = 0.1521, 1.0988, 0.5411, respectively) for **2**, and two bands at 557, 373 nm (f = 0.2800, 2.6300, respectively) for **3** (Fig. S3–S5 in ESI†). The major π–π* absorption band for these three compounds between 310 and 420 nm is consistent with the experimental absorption data in toluene. The weak charge transfer band between 450 and 600 nm in the calculated data of compounds **2** and **3** can be also found in the experimental spectra where it is more like a tail.

Thermal behaviour

The thermal stability was determined using thermogravimetric analysis (TGA) in nitrogen gas at a heating rate of 10 °C min^{-1}. The decomposition temperatures (T_d, corresponding to the 5% weight loss) for compounds **1**, **2**, and **3** are 397, 384, and 306 °C, respectively (Fig. S6 in ESI†). Differential scanning calorimetry (DSC) curves were recorded at a heating rate of 10 °C min^{-1} and showed endothermic transitions at 240 °C for **1**, 300 °C for **2** upon heating (Fig. 5), which have been confirmed as melting points by using polarizing optical microscopy (POM). Compound **2** also exhibited another endothermic transition (glass transition) at 260 °C before its melting point. POM measurements disclosed that **2** entered an anisotropic phase at ~290 °C upon heating and a microcrystalline texture was observed (Fig. 6). Broad and weak endothermic transitions (~96 °C for **1** and ~108 °C for **2**) were observed in DSC curves; however, the corresponding phase transitions could not be observed by POM. Compound **3** showed no phase transition from room temperature to T_d.

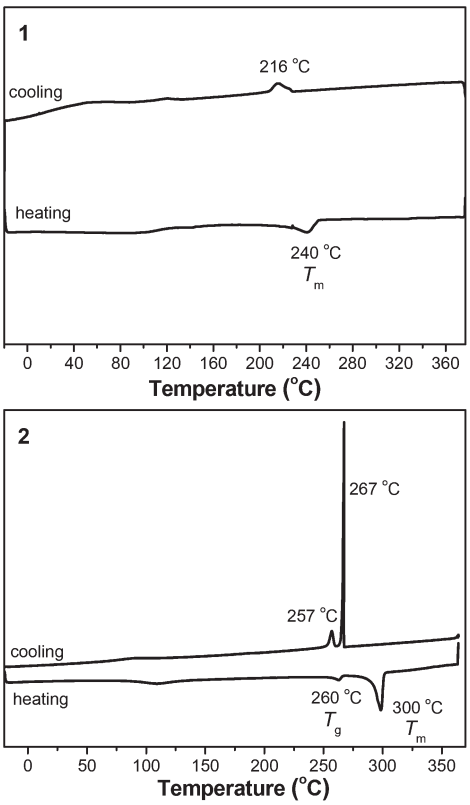

Fig. 5 DSC curves of compounds **1** and **2** (at a heating rate of 10 °C min^{-1} in N_2).

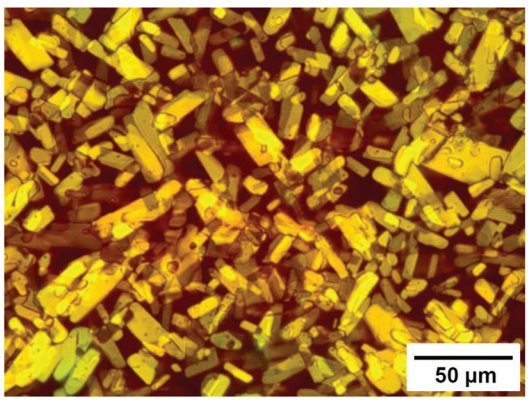

Fig. 6 POM image of **2** at 295 °C upon heating.

Field effect transistors

OFETs were fabricated based on thin films of compounds **1–3** from solution, but only the thin films of **3** showed FET activity. Bottom-gate top-contact FETs were fabricated on p+-Si/SiO_2 substrates by casting a solution of **3** in chlorobenzene (0.15 wt%) onto octadecyltrichlorosilane (OTS) treated substrates. Au source and drain electrodes (80 nm) were patterned on the organic layer through a shadow mask. The as-spun thin film devices were characterized under a N_2 atmosphere or in air. The typical transfer and output curves measured in N_2 are

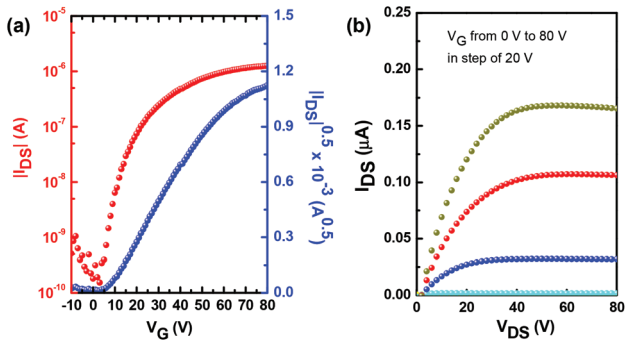

Fig. 7 (a) Output and (b) transfer characteristics of FET devices fabricated by casting a solution of **3** in chlorobenzene on OTS-treated substrates and measured in N_2.

shown in Fig. 7. The device operated in the n-channel region and revealed an average charge carrier mobility of 0.005 cm^2 V^{-1} s^{-1} in the saturation region. The current on/off ratio was about 10^4, and the threshold voltage was around 10 V. When the device was exposed to air, it still showed an electron mobility of 0.001 cm^2 V^{-1} s^{-1}, indicating a relatively good air stability. This behaviour may be owing to the cyano groups in **3** which increase the electron affinity of the molecules and enhance the intermolecular association in the solid state.[5,18] The thin film morphology and microstructure were characterized by the use of tapping-mode atomic force microscopy (AFM) and two-dimensional X-ray diffraction (2D XRD). The thin film exhibited fibrous crystals but with a scatter of grains with a size larger than several microns (Fig. 8c, roughness: 18.1 nm). The XRD pattern (Fig. S7 in ESI†) of the thin film exhibited one major reflection in the small angle region (2θ = 4.27°, *d*-value = 20.7 Å), one weak reflection (2θ = 8.53°, *d*-value = 10.4 Å), and a halo in the wide angle region (2θ > 25°), indicating a dense layer-like packing of the molecules on the substrate.

The AFM measurements on the thin film of **1** (casting from a chlorobenzene solution) displayed an inhomogeneous morphology with a high roughness of 70.5 nm (Fig. 8a). The reason may be attributed to the poor solubility of **1** at room temperature, which hinders the generation of a homogeneous film. XRD pattern of the film only showed one weak reflection at 2θ = 6.55° (*d*-value = 13.5 Å) (Fig. S7 in ESI†), indicating a disordered structure. The AFM image of the thin film of **2** was much more homogeneous. It exhibited large plate-like crystals and gave a surface roughness of 5.92 nm (Fig. 8b). However, the corresponding XRD pattern only showed one reflection peak at 2θ = 4.80° (*d*-value = 18.4 Å, Fig. S7 in ESI†) and the intermolecular packing structure cannot be determined. The low molecular order in **1** and **2** may explain their FET inactivity.

Conclusions

In summary, three BAPQ based derivatives **1–3** with different substituents were synthesized and their physical properties

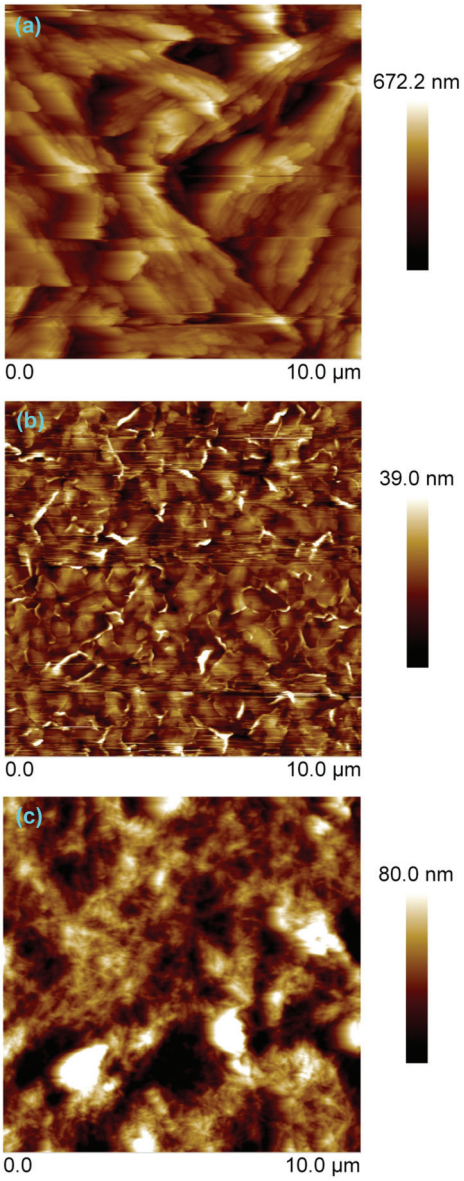

Fig. 8 AFM height images of thin films of (a) **1**, (b) **2**, and (c) **3** on an OTS modified SiO_2 substrate.

were studied in detail. During the synthesis, a new route was developed for the first time to prepare the dialkylated acenaphthenequinone **8**. Compared with the reported mono-alkylated acenaphthenequinone,[19] our dialkylated one is symmetric and hence can control the regularity of the product. The *meso*-substitution with alkylphenyl groups is a more efficient way to improve the solubility of these highly aggregated pyrazinacene compounds. Owing to the attachment of four cyano groups, compound **3** shows a very low-lying LUMO and improved LUMO distribution.[5] The field effect electron mobility of 0.005 cm^2 V^{-1} s^{-1} under a nitrogen atmosphere (0.001 cm^2 V^{-1} s^{-1} in air) was measured from the solution-cast films of **3**. This also represents one of the few examples of pyrazinacenes showing FET activity through solution processing.

Experimental section

General

Anhydrous tetrahydrofuran (THF) was obtained by distillation with sodium. 5,6-Dibromoacenaphthylene-1,2-dione (**4**),[10] 1,2,4,5-tetraaminobenzene tetrahydrochloride (**9**),[11] 4,7-dibromo-5,6-dinitrobenzo[*c*][1,2,5]thiadiazole (**10**),[12] 4-nonylphenyl(trimethyl)stannane (**11**)[13] and 5,6-dicyano acenaphthenequinone (**14**)[14] were prepared according to the reported methods. All other chemicals were purchased from commercial supplies and used without further purification. ^{1}H NMR and ^{13}C NMR spectra were recorded using a Bruker DRX-300 MHz spectrometer or DRX-500 MHz spectrometer in $CDCl_3$ or in $CDCl_2CDCl_2$ at 75 °C. All chemical shifts are quoted in ppm, relative to tetramethylsilane. The residual solvent peak is used as a reference standard. MALDI-TOF mass spectra were recorded using a Bruker MALDI mass spectrometer with 1,8,9-trihydroxy anthracene as the matrix. UV-Vis absorption and fluorescence spectra were recorded using a SHIMADZU UV-1700 UV-Vis spectrometer and a SHIMADZU RF-5301PC fluorometer, respectively. Cyclic voltammetry was performed on a CH Instrument 620C electrochemical analyzer with a three-electrode cell in a solution of 0.1 M tetrabutylammonium hexafluorophosphate (Bu_4NPF_6) in HPLC grade chlorobenzene with a scan rate of 50 mV s^{-1}. A gold electrode with a diameter of 2 mm, a Pt wire and an AgCl/Ag electrode was used as the working electrode, counter electrode and reference electrode, respectively. The potential was then calibrated against the ferrocenium/ferrocene couple. TGA and DSC measurements were performed at a heating rate of 10 °C min^{-1} under nitrogen flow on a TA Instruments SDT 2960 and a METTLER TOLEDO DSC1, respectively. The POM platform was the OLYMPUS BX51, cooperated with a LINKAM TP94 as a thermal control. Tapping-mode atomic force microscopy (TM-AFM) was performed on a Nanoscope V microscope (Veeco Inc.). X-ray diffraction (XRD) patterns of the thin film were measured on a Bruker-AXS D8 DISCOVER with a GADDS X-ray diffractometer. Copper K_α line was used as a radiation source.

Device fabrication

Top-contact, bottom-gate FET devices were prepared on the p+ silicon wafer. A 200 nm thermal SiO_2 layer serves as the gate dielectric. The SiO_2/Si substrate was cleaned with acetone and isopropanol, then immersed in a piranha solution for 8 minutes, followed by rinsing with deionized water, and then re-immersed in a 3 mM solution of octadecyltrichlorosilane (OTS) in hexadecane at rt for 16 h in N_2. It was then rinsed with $CHCl_3$, IPA, DI water and then blow dried with nitrogen gas. The semiconductor layer was deposited on top of the OTS-modified dielectric surface by solution-casting from the solution of compound **3** in chlorobenzene (0.15 wt%). Subsequently, gold source/drain electrodes were deposited by thermal evaporation through a metal shadow mask to create a series of FETs with channel (W = 1 mm, L = 100 nm). The FET devices were then characterized using a Keithley SCS-4200 semiconductor parameter analyzer in the N_2 glove box or in air. To minimize leakage currents, small trenches in the thin film around the electrodes were created with a needle. The FET mobility was extracted using the following equation in the saturation regime from the gate sweep: $I_D = W/(2L)C_i\mu(V_G - V_T)^2$, where I_D is the drain current, μ is the field-effect mobility, C_i is the capacitance per unit area of the gate dielectric layer (SiO_2, 200 nm, C_i = 17 nF cm^{-2}), and V_G and V_T are gate voltage and threshold voltage, respectively. W and L are respectively the channel width and length.

Synthesis and characterization

1,2-Di(1,3-dioxolan-2-yl)-5,6-dibromoacenaphthylene (5). A suspension of 5,6-dibromoacenaphthenequinone **4** (11.8 g, 34.71 mmol), ethylene glycol (30 mL) and 4-methylbenzenesulfonic acid (1.20 g, 6.94 mmol) in dry toluene (100 mL) was refluxed for three days. The resulting water was removed from the reaction by means of a water separator. More ethylene glycol (30 mL) and 4-methylbenzenesulfonic acid (1.20 g, 6.94 mmol) were added to the reaction system every 24 h. After the reaction was completed, the solvent was evaporated and the crude product was extracted from the residue using chloroform (50 mL × 6). Chloroform was removed under reduced pressure to give a crude product, which was washed with ethanol to afford a light brown compound **5** (6.80 g, 45% yield). ^{1}H NMR (500 MHz, $CDCl_3$) δ ppm = 8.01 (d, J = 7.6 Hz, 2H), 7.40 (d, J = 7.6 Hz, 2H), 4.17 (m, 4H), 3.69 (m, 4H); ^{13}C NMR (125 MHz, $CDCl_3$) δ ppm = 138.4, 138.1, 136.2, 127.7, 120.9, 119.3, 97.9, 61.7; Anal. Calcd for $C_{16}H_{12}Br_2O_4$: C, 44.89; H, 2.83; found: C, 44.92; H, 2.73.

1,2-Di(1,3-dioxolan-2-yl)-5,6-di(tetradec-1-ynyl)acenaphthylene (6). Tetradec-1-yne (3.8 g, 19.62 mmol) was injected into a suspension of compound **5** (3.5 g, 8.18 mmol), $Pd(PPh_3)_2Cl_2$ (288 mg, 0.41 mmol), CuI (156 mg, 0.82 mmol) and triethylamine (4.1 g, 5.7 mL) in dry THF (20 mL) under the protection of argon. The mixture was stirred at 75 °C for two days. After cooling to room temperature, the mixture was extracted using ethyl acetate (EA) (50 mL × 3), subsequently washed with deionized water (50 mL × 2) and dried over anhydrous magnesium sulphate. The solvent was removed under reduced pressure and the residue was purified by silica gel column chromatography (silica gel, hexane : EA = 15 : 1) to give a pure compound **6** (4.1 g, 77% yield) as white crystals. ^{1}H NMR (300 MHz, $CDCl_3$) δ ppm = 7.74 (d, J = 7.2 Hz, 2H), 7.46 (d, J = 7.2 Hz, 2H), 4.15 (m, 4H), 3.69 (m, 4H), 2.52 (t, J = 7.1 Hz, 4H), 1.67 (m, 4H), 1.46 (m, 4H), 1.27 (m, 32H), 0.88 (t, J = 6.9 Hz, 6H); ^{13}C NMR (75 MHz, $CDCl_3$) δ ppm = 137.1, 135.9, 135.4, 129.5, 121.5, 119.1, 98.4, 97.4, 79.7, 61.7, 31.9, 29.7, 29.6, 29.3, 29.2, 28.9, 22.7, 20.3, 14.1; Anal. Calcd for $C_{44}H_{62}O_4$: C, 80.69; H, 9.54; found: C, 80.38; H, 9.56; MALDI-TOF MS: 655.340 $[M + H]^+$; calculated exact mass: 654.465.

5,6-Ditetradecylacenaphthenequinone (7). Palladium (on active carbon, 400 mg) was added to a suspension of compound **6** (2.79 g, 4.26 mmol) in ethanol (250 mL) and hydrazine monohydrate (30 mL). The mixture was then stirred at reflux temperature under the protection of argon for two days.

After cooling to room temperature, the mixture was filtered through a thin pad of Celite. The organic solvent of the filtrate was removed under reduced pressure to form an opaque or suspension of the crude product in hydrazine hydrate. It was extracted using hexane or EA (50 mL × 2) and then washed with water (30 mL × 5). Recrystallization from hexane/EA/ethanol gave a pure compound **7** (970 mg, 34% yield) as clear white crystals. ^{1}H NMR (500 MHz, $CDCl_3$) δ ppm = 7.45 (d, J = 7.0 Hz, 2H), 7.39 (d, J = 7.0 Hz, 2H), 4.17 (m, 4H), 3.71 (m, 4H), 3.09 (t, J = 7.6 Hz, 4H), 1.66 (m, 4H), 1.46 (m, 4H), 1.34–1.26 (m, 40H), 0.88 (t, J = 7.0 Hz, 6H); ^{13}C NMR (125 MHz, $CDCl_3$) δ ppm = 140.5, 137.5, 136.0, 130.1, 129.0, 118.8, 98.6, 61.7, 36.1, 33.4, 31.9, 29.8, 29.7, 29.6, 29.5, 29.4, 22.7, 14.1; Anal. Calcd for $C_{44}H_{70}O_4$: C, 79.71; H, 10.64; found: C, 79.34; H, 10.98; MALDI-TOF MS: 663.424 $[M + H]^+$; calculated exact mass: 662.527.

5,6-Ditetradecylacenaphthenequinone (8). A solution of 4-methylbenzenesulfonic acid (2.5 g, 14.5 mmol) in acetonitrile (22 mL) and water (7 mL) was added to the solution of compound **7** (960 mg, 1.45 mmol) in dichloromethane (DCM). The mixture was then stirred at 80 °C overnight. After cooling to room temperature, the organic solvent was removed under reduced pressure. Filtration was done to collect the residue, which was washed with water to give a pure compound **8** in nearly quantitative yield as a yellow solid. ^{1}H NMR (500 MHz, $CDCl_3$) δ ppm = 8.01 (d, J = 7.6 Hz, 2H), 7.62 (d, J = 7.6 Hz, 2H), 3.24 (t, J = 7.6 Hz, 4H), 1.71 (m, 4H), 1.49 (m, 4H), 1.35–1.26 (m, 40H), 0.88 (t, J = 6.9 Hz, 6H); ^{13}C NMR (125 MHz, $CDCl_3$) δ ppm = 188.8, 148.4, 148.3, 130.6, 129.0, 128.2, 121.8, 37.0, 33.0, 31.9, 29.7, 29.6, 29.5, 29.3, 22.7, 14.1; Anal. Calcd for $C_{40}H_{62}O_2$: C, 83.56; H, 10.87; found: C, 83.32; H, 10.64; MALDI-TOF MS: 575.311 $[M + H]^+$; calculated exact mass: 574.475.

BAPQ derivative 1. 5,6-Ditetradecyl acenaphthenequinone **8** (150 mg, 0.26 mmol) and 1,2,4,5-tetraaminobenzene tetrahydrochloride **9** (32 mg, 0.11 mmol) were mixed together in oxygen-free acetic acid (8 mL). The mixture was then stirred at 60 °C for three hours under the protection of argon. After cooling to room temperature, the reaction mixture was filtered to give a yellow solid which was then washed with chloroform and ethanol. Recrystallization from toluene was carried out to afford a pure product **1** (100 mg, 70% yield). ^{1}H NMR (500 MHz, $CDCl_2CDCl_2$, 100 °C) δ ppm = 9.07 (s, 2H), 8.47 (d, J = 7.5 Hz, 4H), 7.74 (d, J = 7.5 Hz, 4H), 3.40 (t, J = 7.5 Hz, 8H), 1.90 (m, 8H), 1.61 (m, 8H), 0.96 (m, 80H), 0.95 (t, J = 6.5 Hz, 12H); ^{13}C NMR (125 MHz, $CDCl_2CDCl_2$, 100 °C) δ ppm = 130.6, 128.8, 121.5, 36.3, 32.7, 31.6, 29.5, 29.4, 29.3, 29.0, 22.3, 13.6; Anal. Calcd for $C_{86}H_{126}N_4$: C, 84.95; H, 10.44; N, 4.61; found: C, 84.73; H, 10.21; N, 4.79; MALDI-TOF MS: 1217.240 $[M + 2H]^+$; calculated exact mass: 1214.998.

5,6-Dinitro-4,7-bis(4-nonylphenyl)benzo[*c*][1,2,5] thiadiazole (12). $Pb(PPh_3)_4$ (58 mg, 0.051 mmol) was added to a solution of 4,7-dibromo-5,6-dinitrobenzo[*c*][1,2,5]thiadiazole **10** (197 mg, 0.51 mmol) and 4-nonylphenyl(trimethyl)stannane **11** (754 mg, 2.05 mmol) in dry THF (10 mL) under the protection of argon. The mixture was stirred at 75 °C for 20 h. After cooling to room temperature, the reaction mixture was treated with a solution of KF in methanol. The mixture was extracted using EA (15 mL × 3) and then washed with deionized water (30 mL × 2) and dried over anhydrous magnesium sulphate. After the solvent was removed under reduced pressure, the residue was purified by column chromatography (silica gel, hexane : EA = 20 : 1) to give a pure compound **12** (230 mg, 71% yield) as a yellow solid. ^{1}H NMR (500 MHz, $CDCl_3$) δ ppm = 7.49 (d, J = 8.2 Hz, 4H), 7.37 (d, J = 8.2 Hz, 4H), 2.71 (t, J = 7.6 Hz, 4H), 1.69 (m, 4H), 1.40–1.29 (m, 24H), 0.89 (t, J = 7.6 Hz, 6H); ^{13}C NMR (125 MHz, $CDCl_3$) δ ppm = 153.1, 145.7, 142.5, 129.1, 129.0, 128.9, 127.6, 35.9, 31.9, 31.1, 29.5, 29.4, 29.3, 22.7, 14.1; Anal. Calcd for $C_{36}H_{46}N_4O_4S$: C, 68.54; H, 7.35; N, 8.88; S, 5.08; found: C, 68.44; H, 7.24; N, 8.54; S, 4.94; MALDI-TOF MS: 630.401 $[M]^-$; calculated exact mass: 630.324.

BAPQ derivative 2. Zn powder (207 mg, 3.2 mmol) was added to a suspension of compound **12** (100 mg, 0.16 mmol) in oxygen free acetic acid (8 mL). The mixture was then stirred at 65 °C under the protection of argon to generate tetraamine **13**. After one hour, the reaction mixture became a white suspension. It was allowed to be stirred at the same temperature for several more hours until nearly all the Zn powder was consumed. The suspension was then cooled to room temperature and the acenaphthenequinone **14a** (29 mg, 0.16 mmol) was added. The mixture was stirred for 30 min to generate the intermediate diamine **15**. Without further separation or purification, the mixture was charged with another equivalent of **14a** (29 mg, 0.16 mmol) and then stirred at 60 °C for 3 h. After cooling to room temperature, the mixture was filtered off and the solid was washed with ethanol. Further purification by column chromatography (silica gel, hexane : chloroform = 2 : 1) afforded a pure product **2** (62 mg, 46% yield) as an orange solid. ^{1}H NMR (500 MHz, CDCl3) δ ppm = 8.31 (d, J = 7.0 Hz, 4H), 8.05 (d, J = 7.6 Hz, 4H), 7.85 (d, J = 8.2 Hz, 4H), 7.78 (t, J = 7.6 Hz, 4H), 7.50 (d, J = 7.6 Hz, 4H), 2.89 (t, J = 7.6 Hz, 4H), 1.89 (m, 4H), 1.50–1.35 (m, 24H), 0.93 (t, J = 7.0 Hz, 6H); ^{13}C NMR (125 MHz, $CDCl_3$) δ ppm = 153.9, 141.9, 139.3, 138.3, 138.2, 133.8, 132.8, 132.1, 130.1, 129.3, 128.5, 127.1, 122.2, 36.2, 32.0, 31.6, 29.7, 29.4, 22.7, 14.1; Anal. Calcd for $C_{60}H_{58}N_4$: C, 86.29; H, 7.00; N, 6.71; found: C, 86.23; H, 7.01; N, 6.63; MALDI-TOF MS: 837.657 $[M + 3H]^+$; calculated exact mass: 834.466.

Compound 16. Zn powder (100 mg, 1.52 mmol) was added to a suspension of compound **12** (40 mg, 0.0634 mmol) in oxygen-free acetic acid (3 mL). The mixture was then stirred at 65 °C under the protection of argon to generate tetraamine **13**. After 3 h, the suspension was cooled to room temperature and 0.7 equivalent of 5,6-dicyano acenaphthenequinone **14b** (10 mg, 0.0444 mmol) was added and the mixture was then stirred for 30 min to give the intermediate diamine **16**. After mixing with water, the mixture was filtered off to obtain a solid. The crude product was extracted using chloroform and then purified through column chromatography (silica gel, chloroform) to give a crude product **16** (13 mg, 28% yield) as a brown solid. Intermediate **16** was not stable enough to be exposed to air for a long time. MALDI-TOF MS: 738.840 $[M]^-$; calculated exact mass: 738.441.

BAPQ derivative 3. A suspension of freshly prepared intermediate diamine **16** (13 mg, 0.0176 mmol) and 5,6-dicyano acenaphthenequinone **14** (4 mg, 0.0176 mmol) in oxygen-free acetic acid (3 mL) was stirred at 60 °C under the protection of argon for 3 h. After cooling to room temperature, the mixture was filtered off. The solid was washed with ethanol and further purified by column chromatography (silica gel, chlorobenzene : THF = 100 : 1) to give a pure product **3** (8 mg, in 48% yield) as a dark red solid. ^{1}H NMR (500 MHz, $CDCl_2CDCl_2$, 75 °C) δ ppm = 8.39 (d, J = 7.5 Hz, 4H), 8.34 (d, J = 7.5 Hz, 4H), 7.78 (d, J = 7.5 Hz, 4H), 7.52 (d, J = 7.5 Hz, 4H), 2.92 (t, J = 8.0 Hz, 4H), 1.93 (m, 4H), 1.60–1.39 (m, 24H), 0.96 (t, J = 7.0 Hz, 6H); ^{13}C NMR (125 MHz, $CDCl_2CDCl_2$, 75 °C) δ ppm = 152.3, 139.0, 136.9, 133.4, 126.9, 122.3, 115.2, 110.2, 35.9, 31.8, 31.1, 29.5, 29.2, 22.5, 13.9; Anal. Calcd for $C_{64}H_{54}N_8$: C, 82.20; H, 5.82; N, 11.98; found: C, 82.38; H, 5.73; N, 11.79; MALDI-TOF MS: 934.935 $[M]^-$; calculated exact mass: 934.447.

Acknowledgements

This work was financially supported by the Singapore MOE AcRF grants R-143-000-510-112 and NUS Start Up grant R-143-000-486-133 (C. C.) and KAUST (K.-W. H.).

Notes and references

1 (*a*) A. Maliakal, K. Raghavachari, H. Katz, E. Chandross and T. Siegrist, *Chem. Mater.*, 2004, **16**, 4980; (*b*) S.-H. Chien, M.-F. Cheng, K. C. Lau and W. K. Li, *J. Phys. Chem. A*, 2005, **109**, 7509.

2 (*a*) C. J. Tonzola, M. M. Alam, W. Kaminsky and S. A. Jenekhe, *J. Am. Chem. Soc.*, 2003, **125**, 13548; (*b*) J. Hu, D. Zhang, S. Jin, S. Z. D. Cheng and F. W. Harris, *Chem. Mater.*, 2004, **16**, 4912; (*c*) V. Lemaur, D. A. da SilvaFilho, V. Coropceanu, M. Lehmann, Y. Geerts, J. Piris, M. G. Debije, A. M. van de Craats, K. Senthilkumar, L. D. A. Siebbeles, J. M. Warman, J.-L. Brédas and G. Cornil, *J. Am. Chem. Soc.*, 2004, **126**, 3271; (*d*) S. C. Jones, F. Barlow, B. Domercq, F. Amy, A. Kahn, J.-L. Brédas, B. Kippelen and S. R. Marder, *J. Am. Chem. Soc.*, 2005, **127**, 16358; (*e*) J. Nishida, S. Murakami, H. Tada and Y. Yamashita, *Chem. Lett.*, 2006, 1236; (*f*) T. Kojima, J. Nishida, S. Tokito, H. Tada and Y. Yamashita, *Chem. Commun.*, 2007, 1430; (*g*) B. R. Kaafarani, L. A. Lucas, B. Wex and G. E. Jabbour, *Tetrahedron Lett.*, 2007, **48**, 5995; (*h*) T. Nakagawa, D. Kumaki, J. Nishida, S. Tokito and Y. Yamashita, *Chem. Mater.*, 2008, **20**, 2615; (*i*) D.-C. Lee, K. Jang, K. K. McGrath, R. Uy, K. A. Robins and D. W. Hatchett, *Chem. Mater.*, 2008, **20**, 3688; (*j*) L. A. Lucas, D. M. DeLongchamp, L. J. Richter, R. J. Kline, D. A. Fischer, B. R. Kaafarani and G. E. Jabbour, *Chem. Mater.*, 2008, **20**, 5743; (*k*) S.-Z. Weng, P. Shukla, M.-Y. Kuo, Y.-C. Chang, H.-S. Sheu, I. Chao and Y.-T. Tao, *ACS Appl. Mater. Interfaces*, 2009, **1**, 2071; (*l*) Z. Liang, Q. Tang, J. Xu and Q. Miao, *Adv. Mater.*, 2011, **23**, 1535; (*m*) Z. Liang, Q. Tang, R. Mao, D. Liu, J. Xu and Q. Miao, *Adv. Mater.*, 2011, **23**, 5514; (*n*) Y.-Y. Liu, C.-L. Song, W.-J. Zeng, K.-G. Zhou, Z.-F. Shi, C.-B. Ma, F. Yang, H.-L. Zhang and X. Gong, *J. Am. Chem. Soc.*, 2010, **132**, 16349.

3 (*a*) J.-I. Nishida, N. Naraso, S. Murai, E. Fujiwara, H. Tada, M. Tomura and Y. Yamashita, *Org. Lett.*, 2004, **6**, 2007; (*b*) E. Ahmed, T. Earmme, G. Ren and S. A. Jenekhe, *Chem. Mater.*, 2010, **22**, 5786; (*c*) J. Shao, J. Chang and C. Chi, *Org. Biomol. Chem.*, 2012, **10**, 7045; (*d*) H. Herrera, P. Echegaray, M. Urdanpilleta, M. J. Mancheno, E. M. Osteritz, P. Bäuerle and J. L. Segura, *Chem. Commun.*, 2013, **49**, 713; (*e*) Q. Ye, J. Chang, K.-W. Huang, X. Shi, J. Wu and C. Chi, *Org. Lett.*, 2013, **15**, 1194.

4 Recent reviews: (*a*) Q. Miao, *Synlett*, 2012, 326; (*b*) C. Wang, H. Dong, W. Hu, Y. Liu and D. Zhu, *Chem. Rev.*, 2012, **112**, 2208.

5 M. Winkler and K. N. Houk, *J. Am. Chem. Soc.*, 2007, **129**, 1805.

6 (*a*) Q. Tang, J. Liu, H. S. Chan and Q. Miao, *Chem.–Eur. J.*, 2009, **15**, 3965; (*b*) S. Miao, P. v. R. Schleyer, J. I. Wu, K. I. Hardcastle and U. H. F. Bunz, *Org. Lett.*, 2007, **9**, 1073; (*c*) O. Tverskoy, F. Rominger, A. Peters, H.-J. Himmel and U. H. F. Bunz, *Angew. Chem., Int. Ed.*, 2011, **50**, 3557; (*d*) D.-C. Lee, K. Jang, K. K. McGrath, R. Uy, K. A. Robins and D. W. Hatchett, *Chem. Mater.*, 2008, **20**, 3688.

7 (*a*) G. J. Richards, J. P. Hill, N. K. Subbaiyan, F. D. Souza, P. A. Karr, M. R. J. Elsegood, S. J. Teat, T. Mori and K. Ariga, *J. Org. Chem.*, 2009, **74**, 8914; (*b*) C. Tong, W. Zhao, J. Luo, H. Mao, W. Chen, H. S. O. Chan and C. Chi, *Org. Lett.*, 2012, **14**, 494.

8 5,7,12,14-Tetraazapentacene is not stably existent, but the highly stable BAPQ has been reported in a patent: S. Zheng, Z. Jiang, J. Tillema and R. Ramirez, *Patent US* 2011/0026117 A1, 2011.

9 C. R. Newman, C. D. Frisbie, D. A. da Silva Filho, J.-L. Brédas, P. C. Ewbank and K. R. Mann, *Chem. Mater.*, 2004, **16**, 4436.

10 (*a*) N. Tanaka and T. Kasai, *Bull. Chem. Soc. Jpn.*, 1981, **54**, 3020; (*b*) W. D. Neudorff, D. Lentz, M. Anibarro and A. D. Schlüter, *Chem.–Eur. J.*, 2003, **9**, 2745; (*c*) M. Tesmer and H. Vahrenkamp, *Eur. J. Inorg. Chem.*, 2001, 1183.

11 (*a*) G. W. H. Cheeseman, *J. Chem. Soc.*, 1962, 1170; (*b*) K. Wolfgang and N. Hartmut, *Chem. Ber.*, 1958, **91**, 2562.

12 (*a*) A. P. Zoombelt, M. Fonrodona, M. G. R. Turbiez, M. M. Wienk and R. A. J. Janssen, *J. Mater. Chem.*, 2009, **19**, 5336; (*b*) E. Wang, L. Hou, Z. Wang, S. Hellstroem, W. Mammo, F. Zhang, O. Inganaes and M. R. Andersson, *Org. Lett.*, 2010, **12**, 4470.

13 (*a*) T. Mutai, J.-D. Cheon, S. Arita and K. Araki, *J. Chem. Soc., Perkin Trans. 2*, 2001, 1045; (*b*) M. R. Friedman, K. J. Toyne, J. W. Goodby and M. Hird, *Liq. Cryst.*, 2001, **28**, 901.

14 L. Ding, H.-Z. Ying, Y. Zhou, T. Lei and J. Pei, *Org. Lett.*, 2010, **12**, 5522.

15 (*a*) J. Pommerehne, H. Vestweber, W. Guss, R. F. Mahrt, H. Bassler, M. Porsch and J. Daub, *Adv. Mater.*, 1995, **7**, 551; (*b*) C. Chi and G. Wegner, *Macromol. Rapid Commun.*, 2005, **26**, 1532.

16 (*a*) W. J. Hehre, R. Ditchfield and J. A. Pople, *J. Chem. Phys.*, 1972, **56**, 2257; (*b*) C. Lee, W. Yang and R. G. Parr, *Phys. Rev. B: Condens. Matter*, 1988, **37**, 785; (*c*) A. D. Becke, *J. Chem. Phys.*, 1993, **98**, 5648; (*d*) R. Krishnan, J. S. Binkley, R. Seeger and J. A. Pople, *J. Chem. Phys.*, 1980, **72**, 650.

17 M. J. Frish, *et al.*, *Gaussian 09, Revision A.2*, Gaussian, Inc., Wallingford, CT, 2009.

18 (*a*) G. R. Desiraju, *Angew. Chem., Int. Ed. Engl.*, 1995, **34**, 2311; (*b*) G. R. Desiraju, *Chem. Commun.*, 1997, 1475; (*c*) B. A. Jones, M. J. Ahrens, M.-H. Yoon, A. Facchetti, T. J. Marks and M. R. Wasielewski, *Angew. Chem., Int. Ed.*, 2004, **43**, 6363.

19 A. Palmaerts, L. Lutsen, T. J. Cleij, D. Vanderzande, A. Pivrikas, H. Neugebauer and N. S. Sariciftci, *Polymer*, 2009, **50**, 5007.